

STUDY ON SATURATION CONSIDERATION AND ITS INCORPORATION INTO INDUCTION MOTOR MODELLING

Rini Nur Hasanah

ABSTRACT: In common practices, motor inductances are considered constant and not much affected by magnetic saturation associated with various operating conditions. However, saturation might produce either desired or undesired effects. Considering the importance of saturation, it must be accounted for in the machine modeling. However, the saturation problem is not easy to handle. As a result, the accuracy of the machine performance prediction depends on whether the saturation is incorporated into the modeling. This paper presents some approaches to consider magnetic saturation and incorporate it into motor modeling.

Keywords: Induction motor, Magnetic saturation, Motor modeling, Space-phasor

ABSTRAK: Kejenuhan magnetik dapat menimbulkan efek yang dapat merugikan atau sebaliknya bahkan menguntungkan serta diinginkan. Kejenuhan magnetik sangat penting untuk diperhatikan namun tidak mudah untuk ditangani dan dimodelkan. Dalam berbagai kajian penerapan mesin tak serempak, induktansi pada umumnya dianggap konstan dan tidak terpengaruh oleh adanya kejenuhan magnetik yang dapat terjadi dalam berbagai kondisi operasi.. Akibatnya pemodelan mesin tidak menggambarkan kondisi mesin sebenarnya pada saat dioperasikan dengan tingkat kejenuhan tertentu. Tulisan ini mengkaji beberapa pendekatan untuk memperhitungkan tingkat kejenuhan magnetik dalam motor tak serempak serta bagaimana menerapkannya dalam pemodelan motor untuk memperkirakan berbagai karakteristiknya.

Kata-kata kunci: Motor tak serempak, Kejenuhan magnetik, Pemodelan motor, Fasor ruang

Magnetic saturation can take place during various operating conditions of an induction machine. Saturation might produce either desired or undesired effects. In a motor, it can result in undesirable effects, for instance less torque and higher harmonics productions. These effects could result in an uneconomical use of electrical energy. In converter-fed induction motor drives and autonomous induction generators, ignoring the saturation effects could lead to inaccuracy results or even make simulation and performance prediction impossible. On the other hand, a saturated condition is desired in order that a final steady-state voltage can be achieved during the voltage generation in an induction generator.

Considering the importance of saturation, it must be accounted for in the machine modelling. However, the saturation problem is not easy to handle. As a result, the accuracy of the machine

performance prediction depends on whether the saturation is incorporated in the modelling.

Motor parameters which are mostly affected by saturation are the magnetizing and leakage inductances. Some authors (Câmpeanu, 1995; Driscoll, 2002) consider only the saturation in the magnetizing flux path, arguing that it is the steady-state operation condition which deserves the attention. Some others (Ojo, 1998; Keyhani, 1989; Faiz, 1995) consider also the leakage flux path saturation, making possible the prediction of motor transient performance, for example during free acceleration. Ojo emphasized the importance to include the stator core saturation; however the experimental measurement to provide the needed parameters is tedious and involved.

On direct-on-line starting of induction motor, the sudden rise of supplying voltage and current saturates the flux paths in certain parts of motor,

and as the condition is similar to an instantaneous short-circuit, the leakage inductances will be affected much more than the magnetizing inductance. Except for pedagogic purpose, free acceleration of an induction motor has no great importance in regard to practical application. However, it is very useful to understand the saturation phenomenon in general.

INCORPORATING SATURATION INTO MOTOR MODELING

It is taken that stator and rotor fluxes are composed of the main flux and leakage fluxes. Depending on the operating condition, either the main flux or the leakage flux, or both, can be important.

The consequence of magnetizing flux saturation can be known using the no-load tests. The stator and rotor leakage inductances of a saturated induction machine can be obtained by using the Finite Element Method analysis. The consequence of the leakage flux saturation can be determined using the locked rotor tests, but it must be done carefully in the case of deep-bar rotors because inductance will depend not only on the current, but also on the frequency.

Magnetizing Saturation Curve

To incorporate the magnetizing saturation effects, it is supposed that the saturation curve, either the B-H curve or the Ψ -I curve, is known from the data provided by the manufacturer. The curve is used to represent the magnetizing flux dependency on the magnetizing current. Using the magnetizing curve, two kinds of inductance are considered:

- the static inductance, which is the slope of a straight line from the origin through the operating point on the magnetizing curve,

- the dynamic inductance, which is the slope of the tangent line to the magnetizing curve at the operating point.

In order to obtain the static and dynamic inductances, the magnetizing curve obtained from a no-load test should be modeled mathematically. The static and dynamic inductance curves depend on the mathematical model used for the magnetizing curve.

Among various mathematical modelings of the magnetizing curve are the following (Ganji, 1998):

- Arctangent model :

$$\Psi_m = A \tan^{-1}(BI_m) + CI_m \quad (1)$$

It represents the relation between magnetizing flux Ψ_m and current I_m , with A, B and C are constants.

- Levi's model (1994):

$$\Psi_m = A B^m I_m^C \quad (2)$$

It represents the relation between magnetizing flux Ψ_m and current I_m , with A, B and C are constants.

- Exponential model (Ganji, 1998):

$$L_m = A e^{-\frac{I_m}{C}} - B e^{-\frac{I_m}{D}} + E \quad (3)$$

It represents the relation between magnetizing inductance L_m and current I_m , with E is the saturated inductance, whereas A,B,C and D depend on the inductance at zero magnetizing current and the shape of the inductance function. Under this model, low level iron nonlinearity is taken into account.

- Audo's segmented model (1998):

In this model, the data are treated using the so-called segmented

saturation modelling. The magnetizing curve is segmented into three parts, each of them represents the low-level nonlinearity, linearity and saturation respectively. Using this model, relationship between the two curve components can be expressed in both directions. However, there is a difficulty in determining three points to construct as real as possible the magnetizing curve. Very often, many trial-and-error attempts have to be made before arriving at the desired curve form. The three points to determine are (Fig. 1):

- (H_1, B_1) representing the smallest B amplitude
- (H_2, B_2) representing the middle of the curve knee
- (H_3, B_3) representing the highest B amplitude, corresponding more or less to the straight saturated part

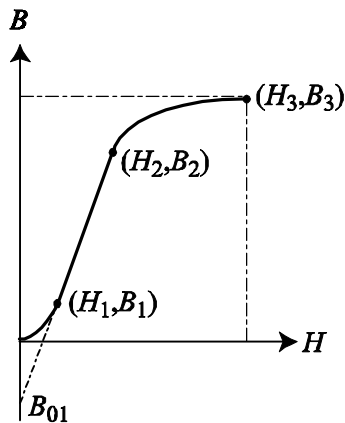


Figure 1 B-H curve segmentation (Audo, 1998)

If the Audo's method is used to approximate the magnetization curve of machine B given in Table 1, the result is shown in Fig. 2. The curves of flux linkage, static L_m and dynamic inductance L as functions of magnetizing current I_m are shown. The dynamic inductance is given as:

$$L = \frac{d\Psi_m}{dI_m} \tag{4}$$

whereas the static inductance is given as:

$$L_m = \frac{\Psi_m}{I_m} \tag{5}$$

It shows that along the linear part of the flux linkage curve (the saturation has not been reached) the dynamic and static inductances are equal.

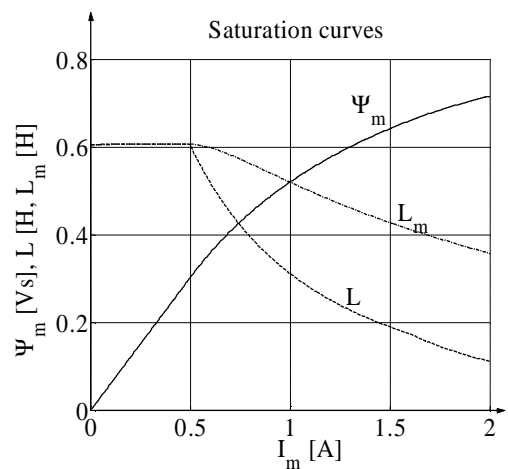


Figure 2 The magnetizing curve of induction machine B (Table 1) and its respective dynamic and magnetizing inductances

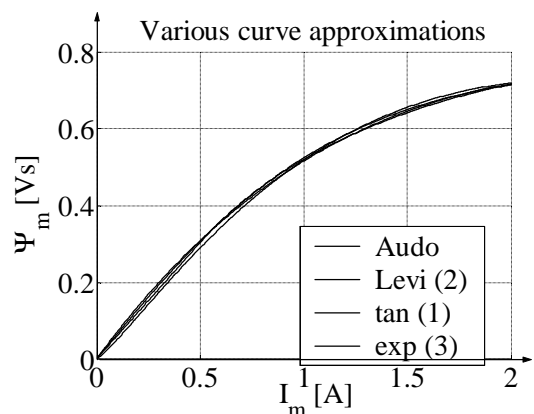


Figure 3 Comparison of various magnetizing curve approximations

When the previous approximations are all applied on the

same magnetizing saturation data, the resulted four curves correspond one another almost identically (Fig. 3). However, the resulted static and dynamic inductances show clear differences, especially on the low level current or flux linkage, as shown in Fig. 4.

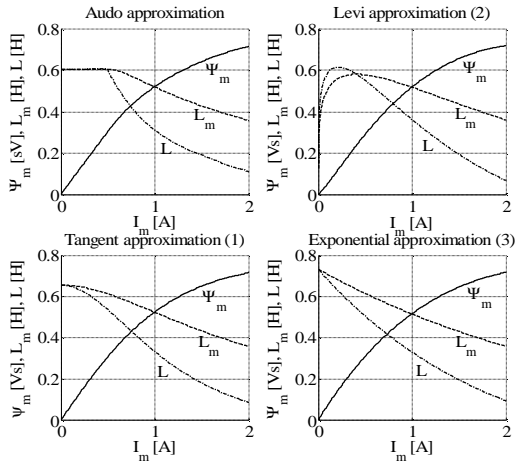


Figure 4 Comparison of various magnetizing curve approximations

Motor Voltage Equations with Saturation

The space-phasor of the magnetizing current expressed in the general reference frame is shown in Fig. 5 (Vas, 1996). The general reference frame $x + jy$ rotates with an angular speed $w_g = \frac{dq_g}{dt}$. The real axis x of the general reference frame has an angle q_g with respect to the real axis of the stationary stator frame s_D . The magnetizing current space-phasor \bar{i}_{mg} has an angle r_m with respect to the real axis of the stationary stator frame, and $(r_m - q_g)$ with respect to the general reference frame.

The magnetizing current space-phasor:

$$\bar{i}_{mg} = |\bar{i}_m| e^{j(r_m - q_g)} \tag{6}$$

where $r_m - q_g = \tan^{-1}\left(\frac{i_{my}}{i_{mx}}\right)$ (7)

and $|\bar{i}_m| = \sqrt{i_{mx}^2 + i_{my}^2}$ (8)

The angle $(r_m - q_g)$ represents the cross-saturation coupling between windings in space quadrature. The cross-saturation coupling inductance is:

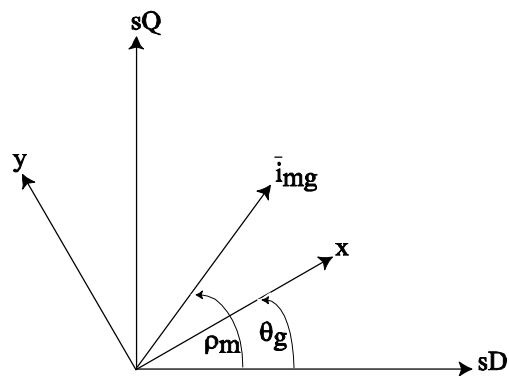


Figure 5 The space-phasor of the magnetizing current expressed in the general reference frame

$$L_{xy} = (L - L_m) \sin r_m \cos r_m \tag{9}$$

where the dynamic inductance is:

$$L = \frac{d|\bar{y}_{mg}|}{d|\bar{i}_{mg}|} \tag{10}$$

and the static (magnetizing) inductance is:

$$L_m = \frac{|\bar{y}_{mg}|}{|\bar{i}_{mg}|} \tag{11}$$

Here, $|\bar{y}_{mg}| = \sqrt{y_{mx}^2 + y_{my}^2}$ and $|\bar{i}_{mg}| = \sqrt{i_{mx}^2 + i_{my}^2}$ are the moduli of the magnetizing flux linkage and current space-phasor respectively.

L_{xy} is zero under linear magnetic conditions because $L = L_m$ does not

depend on the magnetizing current, oppositely under saturated conditions where $L \neq L_m$ and both depend on the magnetizing current.

To incorporate the saturation effect, we start from the stator and rotor voltage equations in the general reference frame:

$$\begin{aligned} \bar{u}_{sg} &= u_{sx} + ju_{sy} \\ &= R_s \bar{i}_{sg} + L_{ls} \frac{d\bar{i}_{sg}}{dt} + \frac{d\bar{y}_{mg}}{dt} \\ &\quad + jw_g (L_{ls} \bar{i}_{sg} + \bar{y}_{mg}) \end{aligned} \quad (12)$$

$$\begin{aligned} \bar{u}_{rg} &= u_{rx} + ju_{ry} \\ &= R_r \bar{i}_{rg} + L_{lr} \frac{d\bar{i}_{rg}}{dt} + \frac{d\bar{y}_{mg}}{dt} \\ &\quad + j(w_g - w_r)(L_{lr} \bar{i}_{rg} + \bar{y}_{mg}) \end{aligned} \quad (13)$$

Magnetizing flux linkage and magnetizing voltage space-phasor in the general reference frame can be developed as:

$$\begin{aligned} \bar{y}_{mg} &= L_m \bar{i}_{mg} \\ &= L_m |\bar{i}_m| e^{j(r_m - q_g)} = L_m (\bar{i}_{sg} + \bar{i}_{rg}) \end{aligned} \quad (14)$$

$$\bar{u}_{mg} = \frac{d\bar{y}_{mg}}{dt} = \frac{d(L_m \bar{i}_{mg})}{dt} \quad (15)$$

Due to saturation, magnetizing inductance L_m is a function of magnetizing current:

$$L_m = \frac{\bar{y}_{mg}}{\bar{i}_{mg}} = \frac{|\bar{y}_{mg}|}{|\bar{i}_{mg}|} = \frac{|\bar{y}_m|}{|\bar{i}_m|} \quad (16)$$

Developing the magnetizing voltage space-phasor into its components results in:

$$\begin{aligned} \bar{u}_{mg} &= u_{mx} + ju_{my} \\ &= \frac{d(y_{mx} + jy_{my})}{dt} = \frac{d(L_m i_{mx} + jL_m i_{my})}{dt} \end{aligned} \quad (17)$$

$$u_{mx} = \frac{dy_{mx}}{dt} = \frac{d(L_m i_{mx})}{dt} = \frac{d(L_m (i_{sx} + i_{rx}))}{dt} \quad (18)$$

$$u_{my} = \frac{dy_{my}}{dt} = \frac{dL_m i_{my}}{dt} = \frac{d(L_m (i_{sy} + i_{ry}))}{dt} \quad (19)$$

Expanding each magnetizing space-phasor component using the chain differentiation rule results in:

$$\begin{aligned} u_{mx} &= \frac{dy_{mx}}{dt} \\ &= \frac{\partial y_{mx}}{\partial i_{mx}} \frac{di_{mx}}{dt} + \frac{\partial y_{mx}}{\partial i_{my}} \frac{di_{my}}{dt} \\ &= L_{mx} \frac{di_{mx}}{dt} + L_{xy} \frac{di_{my}}{dt} \end{aligned} \quad (20)$$

$$\begin{aligned} u_{my} &= \frac{dy_{my}}{dt} \\ &= \frac{\partial y_{my}}{\partial i_{my}} \frac{di_{my}}{dt} + \frac{\partial y_{my}}{\partial i_{mx}} \frac{di_{mx}}{dt} \\ &= L_{my} \frac{di_{my}}{dt} + L_{yx} \frac{di_{mx}}{dt} \end{aligned} \quad (21)$$

Because of saturation, in general $L_{mx} \neq L_{my}$ and $L_{xy} \neq 0$. It follows:

$$\begin{aligned} u_{mx} &= \frac{dy_{mx}}{dt} = \frac{d(L_m i_{mx})}{dt} \\ &= L_m \frac{di_{mx}}{dt} + i_{mx} \frac{dL_m}{dt} \end{aligned} \quad (22)$$

$$\begin{aligned} \frac{dL_m}{dt} &= \frac{dL_m}{d|\bar{i}_m|} \frac{d|\bar{i}_m|}{dt} = \frac{d \frac{|\bar{y}_m|}{|\bar{i}_m|}}{d|\bar{i}_m|} \frac{d|\bar{i}_m|}{dt} \\ &= \frac{|\bar{i}_m| d|\bar{y}_m| - |\bar{y}_m| d|\bar{i}_m|}{|\bar{i}_m|^2} \frac{d|\bar{i}_m|}{dt} \end{aligned} \quad (23)$$

$$\begin{aligned} &= \frac{1}{|\bar{i}_m|} \left(\frac{d|\bar{y}_m|}{d|\bar{i}_m|} - \frac{|\bar{y}_m|}{|\bar{i}_m|} \right) \frac{d|\bar{i}_m|}{dt} \\ &= \frac{(L - L_m) d|\bar{i}_m|}{|\bar{i}_m| dt} \end{aligned}$$

Finally, it gives:

$$u_{mx} = L_m \frac{di_{mx}}{dt} + \frac{i_{mx}}{|i_m|} (L - L_m) \frac{d|i_m|}{dt} \quad (24)$$

where

$$\begin{aligned} \frac{d|i_m|}{dt} &= \frac{d\sqrt{i_{mx}^2 + i_{my}^2}}{dt} \\ &= \frac{1}{2} \frac{2i_{mx} \frac{di_{mx}}{dt} + 2i_{my} \frac{di_{my}}{dt}}{\sqrt{i_{mx}^2 + i_{my}^2}} \\ &= \frac{i_{mx} \frac{di_{mx}}{dt} + i_{my} \frac{di_{my}}{dt}}{|i_m|} = \frac{i_{mx}}{|i_m|} \frac{di_{mx}}{dt} + \frac{i_{my}}{|i_m|} \frac{di_{my}}{dt} \\ &= \cos(r_m - q_g) \frac{di_{mx}}{dt} + \sin(r_m - q_g) \frac{di_{my}}{dt} \end{aligned} \quad (25)$$

The real and imaginary components of magnetizing voltage space-phasor can then be written as:

$$u_{mx} = L_m \frac{di_{mx}}{dt} + \cos(r_m - q_g) (L - L_m) \left[\cos(r_m - q_g) \frac{di_{mx}}{dt} + \sin(r_m - q_g) \frac{di_{my}}{dt} \right] \quad (26)$$

$$= L_m \frac{di_{mx}}{dt} + L_{xy} \frac{di_{my}}{dt}$$

$$u_{my} = L_m \frac{di_{my}}{dt} + \sin(r_m - q_g) (L - L_m) \left[\cos(r_m - q_g) \frac{di_{mx}}{dt} + \sin(r_m - q_g) \frac{di_{my}}{dt} \right] \quad (27)$$

$$= L_{my} \frac{di_{my}}{dt} + L_{xy} \frac{di_{mx}}{dt}$$

where

$$L_{mx} = L_m + (L - L_m) \cos^2(r_m - q_g) \quad (28)$$

$$L_{my} = L_m + (L - L_m) \sin^2(r_m - q_g) \quad (29)$$

$$L_{xy} = (L - L_m) \frac{\sin 2(r_m - q_g)}{2} \quad (30)$$

Finally, the direct- and quadrature-axis components of the stator and rotor voltage equations become:

$$u_{sx} = R_s i_{sx} + L_{sx} \frac{di_{sx}}{dt} + L_{xy} \frac{di_{sy}}{dt} - w_g L_s i_{sy} + L_{mx} \frac{di_{rx}}{dt} + L_{xy} \frac{di_{ry}}{dt} - w_g L_m i_{ry} \quad (31)$$

$$u_{sy} = L_{xy} \frac{di_{sx}}{dt} + w_g L_s i_{sx} + R_s i_{sy} + L_{sy} \frac{di_{sy}}{dt} + L_{xy} \frac{di_{rx}}{dt} + w_g L_m i_{rx} + L_{my} \frac{di_{ry}}{dt} \quad (32)$$

$$u_{rx} = L_{mx} \frac{di_{sx}}{dt} - (w_g - w_r) L_m i_{sy} + L_{xy} \frac{di_{sy}}{dt} + R_r i_{rx} + L_{rx} \frac{di_{rx}}{dt} - (w_g - w_r) L_r i_{ry} + L_{xy} \frac{di_{ry}}{dt} \quad (33)$$

$$u_{ry} = (w_g - w_r) L_m i_{sx} + L_{xy} \frac{di_{sx}}{dt} + L_{my} \frac{di_{sy}}{dt} + (w_g - w_r) L_r i_{rx} + L_{xy} \frac{di_{rx}}{dt} + R_r i_{ry} + L_{ry} \frac{di_{ry}}{dt} \quad (34)$$

or in a matrix form as follows:

$$\begin{bmatrix} u_{sx} \\ u_{sy} \\ u_{rx} \\ u_{ry} \end{bmatrix} = \begin{bmatrix} R_s + L_{sx} p & L_{xy} p - w_g L_s & L_{mx} p & L_{xy} p - w_g L_m \\ L_{xy} p + w_g L_s & R_s + L_{sy} p & L_{xy} p + w_g L_m & L_{my} p \\ L_{mx} p & L_{xy} p - (w_g - w_r) L_m & R_r + L_{rx} p & L_{xy} p - (w_g - w_r) L_r \\ L_{xy} p + (w_g - w_r) L_m & L_{my} p & L_{xy} p + (w_g - w_r) L_r & R_r + L_{ry} p \end{bmatrix} \begin{bmatrix} i_{sx} \\ i_{sy} \\ i_{rx} \\ i_{ry} \end{bmatrix} \quad (35)$$

where

$$L_{sx} = L_{ls} + L_{mx}, \quad L_{sy} = L_{ls} + L_{my},$$

$$L_s = L_{ls} + L_m \quad (36)$$

$$L_{rx} = L_{lr} + L_{mx}, \quad L_{ry} = L_{lr} + L_{my},$$

$$L_r = L_{lr} + L_m \quad (37)$$

In the state-variable form, using currents as state variables, the voltage equations have almost the same forms as in the case without saturation, with a different form of inductance matrix which does not contain zero elements.

Following is the comparison between the inductance matrix with and

without saturation consideration (Vas, 1996; Krause, 1995):

$$\mathbf{L}_{\text{unsaturated}} = \begin{bmatrix} L_s & 0 & L_m & 0 \\ 0 & L_s & 0 & L_m \\ L_m & 0 & L_r & 0 \\ 0 & L_m & 0 & L_r \end{bmatrix} \quad (38)$$

$$\mathbf{L}_{\text{saturated}} = \begin{bmatrix} L_{sx} & L_{xy} & L_{mx} & L_{xy} \\ L_{xy} & L_{sy} & L_{xy} & L_{my} \\ L_{mx} & L_{xy} & L_{rx} & L_{xy} \\ L_{xy} & L_{my} & L_{xy} & L_{ry} \end{bmatrix} \quad (39)$$

L_{xy} is called the cross-saturation coupling inductance, and is zero whenever $r_m = q_g$.

When the flux linkage is used as state variable, there is an advantage of taking into account only the static magnetizing inductance, however the anisotropies (asymmetries) caused by saturation cannot be observed easily because it is concealed in the equations (Vas, 1996). The equations used are the same as those without considering the saturation, oppositely to using currents as state variables.

INFLUENCE OF SATURATION ON MOTOR CHARACTERISTICS

Motor characteristics with magnetizing saturation consideration are obtained using (7)-(9), (14)-(16) combined with the motor equation of motion as follows:

$$\frac{dw_r}{dt} = \frac{p}{J} \frac{3}{2} (T_e - T_L) \quad (40)$$

and the torque equation:

$$T_e = \frac{3}{2} p L_m (i_{sy} i_{rx} - i_{sx} i_{ry}) \quad (41)$$

The dynamic and static inductances L and L_m vary according to the value of

magnetizing current i_m . The inductance variation can be approximated, for example by using (1), (2), (3) or the approach proposed by Audo et al. (1986).

SIMULATION RESULTS

Considering Only the Static Inductance

Fig. 6 and Fig. 7 show respectively the evolution of the magnetizing current and static magnetizing inductance with respect to time during the free-acceleration of Motor A (Table 1).

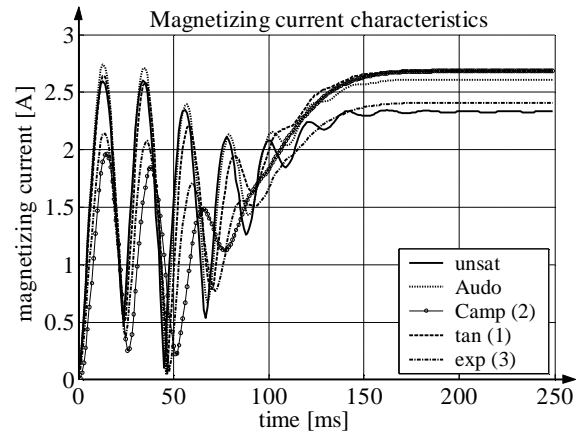


Figure 6 Magnetizing current characteristics of Motor A (Table 1) based on various saturation curve approximations

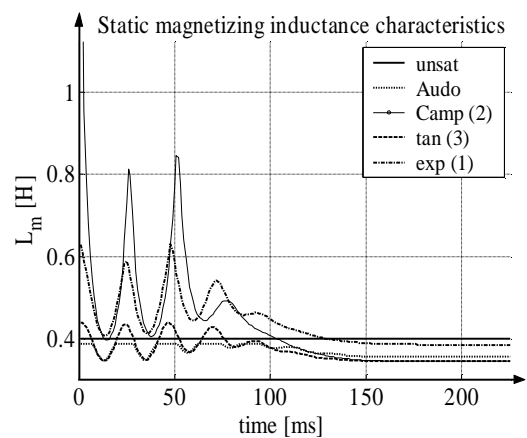


Figure 7 Static magnetizing inductance characteristics of Motor A (Table 1) based on various saturation curve approximations

As shown in Fig. 6 and Fig. 7, the impact of saturation during the transient period depends on the model of the magnetizing curve. Almost identical $\Psi_m - I_m$ curve models can give very different current and inductance evolutions during the transient period.

Fig. 7 shows that using the Audo's approach for Motor A, the static inductance variation during the early moments of acceleration period is not so great as the variations obtained using the three other approximations.

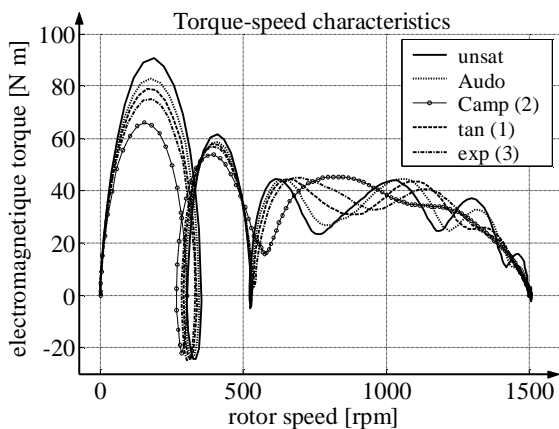


Figure 8 The influence of the static magnetizing inductance saturation on the torque-speed characteristic during the free-acceleration of Motor A

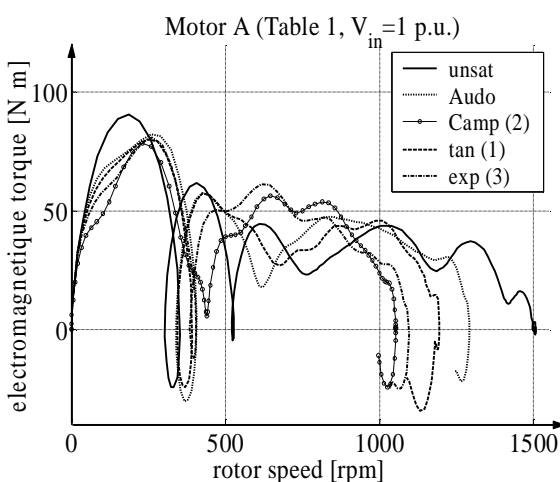


Figure 9 The influence of both the static and dynamic inductances saturation on the torque-speed characteristic during the free-acceleration of Motor A

The characteristic of the electromagnetic torque with respect to rotor speed is shown in Fig. 8. It shows that saturation results in the decrease in the torque oscillation at the beginning of the transient period. In addition, during the transient period there is a large difference between the torques obtained with and without saturation, which is continuing to decrease before finally reaches equal values at steady-state.

Considering both the Static and Dynamic Inductances

The influence of both the static and dynamic inductances saturation on the Motor A (Table 1) is shown in Fig. 9, whereas on the Motor B (Table 1) is shown in Fig. 10. The differences between the two figures are caused by different motor parameters and saturation conditions. In Fig. 9, the similarities in the characteristic forms are due to the level of saturation condition of the motor. It shows that Motor A is not too saturated, oppositely to Motor B.

As shown in Fig. 11, using a lower value of line input voltage, the level of saturation is reduced, so that the resulted torque-speed characteristic is not too different from that without saturation consideration.

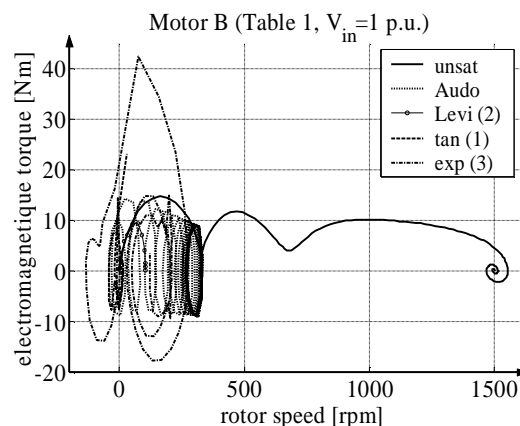


Figure 10 The influence of both the static and dynamic inductances saturation on the torque-speed characteristic during the free-acceleration of Motor B

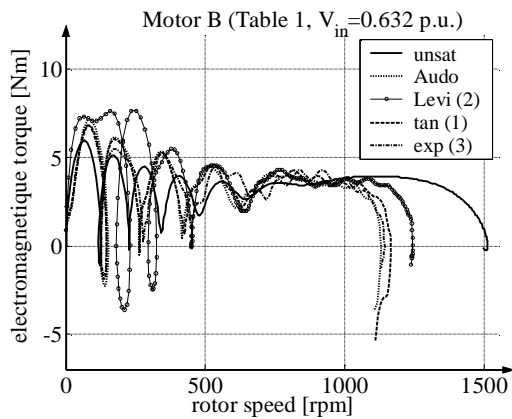


Figure 11 The influence of both the static and dynamic inductances saturation on the torque-speed characteristic during the free-acceleration of Motor B (with line input voltage = 0.632 p.u.)

Fig. 9 shows that including the dynamic inductance saturation could result in very different torque-speed characteristics, as compared to Fig. 8, and again it depends on the motor parameters and saturation level.

Considering the Leakage and Magnetizing Inductances

Incorporating saturation into motor modelling can be done by considering only the saturation of the main flux paths (magnetizing flux paths), or including also the leakage flux paths. The choice priority depends on their importance during motor operation.

The complexity in considering the leakage inductance stems from the difficulty to find the saturation curve using the locked-rotor test, for example:

- when the rotor slot is deep,
- the separation between the stator and rotor leakages, which are normally considered to be equal in case of with no saturation.

To also consider the leakage inductance saturation, the leakage inductance is normally assumed to be divided into a non-saturated (constant) and saturable (iron-dependent) parts (Vas, 1996). The main and leakage flux

paths are usually assumed to be independent of each other, otherwise a functional dependency must be found, for example by using an analytical expression.

CONCLUSION

Integrating saturation into motor modeling is necessary to approach the motor real condition more closely. As the saturation could have either desired or undesired effect, its influence on motor characteristics needs to be analyzed. This consideration is a must mainly during motor design and optimization.

APPENDIX

Table 1 Machine A (Câmpeanu, 1995) and Machine B (Levi, 1994) used in all calculations

Machine	A	B	Unit
Output power	4	0.75	[kW]
Supply voltage	220/380 Δ/Y	220/380 Δ/Y	[V]
Supply frequency	50	50	[Hz]
Phase-number	3	3	[-]
Pole-pairs number	2	2	[-]
Inertia	0.024	0.00442	[kg·m ²]
Stator resistance	1.16	10	[Ω]
Rotor resistance	3.515	6.3	[Ω]
Stator leakage inductance	0.024	0.043067	[H]
Rotor leakage inductance	0.0034	0.04107	[H]
Rated magnetizing inductance	-	0.42119	[H]

Magnetizing curve approximation for machine B in terms of phase r.m.s.

current values is expressed as:

$$\Psi_m = 0.86427 \times 0.59976 I_m^{1.211}$$

BIBLIOGRAPHY

Audo, T. and Umoto, J. (1986). "A 2D numerical solution of transient magnetic flux distribution in electric machines considering magnetic saturation and hysteresis", *Mem. Fac. Eng.*, Kyoto Univ. vol. 48, No. 3.

Câmpeanu, A. (1995). "Transient performance of the saturated induction machine", *Electrical Engineering* 78, pp. 241-241. Springer Verlag.

Driscoll, T.A. *et al.* (2002). *Schwarz-Christoffel Mapping*. Cambridge: Cambridge University Press.

Faiz, Jawad and. Seifi, A.R. (1995). "Dynamic analysis of induction motors with saturable inductances", *Electric Power System Research* 34, pp. 205-210, Elsevier Science S.A.

Ganji, A. *et al.* (1998). "Induction motor dynamic and static inductance identification using a broadband excitation technique", *IEEE Transaction on Energy Conversion*, vol. 13, No. 1, March 1998, pp. 15-20.

Keyhani, A. and Tsai, H. (1989). "IGSPICE Simulation of induction machines with saturable inductances", *IEEE Transactions on Energy Conversion*, Vol. 4, No. 1, March 1989.

Krause, P.C. *et al.* (1995). *Analysis of Electric Machinery*, New York: IEEE Press.

Levi, E. (1994) "Applications of the current state space model in analyses of saturated induction machines", *Electric Power System Research* 31, pp. 203-216, Elsevier Science S.A.

Ojo, J.O. *et al.* (1988). "An improved model of saturated induction machines", *Conference Record IEEE IAS Annual Meeting*, 2-7 Oct 1988, vol. 1, pp. 222-230.

Vas, P. (1996). *Electrical Machines and Drives: A Space-Vector Theory Approach*. Clarendon Press, Oxford.